SELF-SYNCHRONIZATION OF MANY COUPLED OSCILLATORS

by

M. de Sousa Vieira, A. J. Lichtenberg,
and M. A. Lieberman

Memorandum No. UCB/ERL M92/20

26 February 1992

SELF-SYNCHRONIZATION OF MANY COUPLED OSCILLATORS

by

M. de Sousa Vieira, A. J. Lichtenberg,
and M. A. Lieberman

Memorandum No. UCB/ERL M92/20

26 February 1992

ELECTRONICS RESEARCH LABORATORY

College of Engineering
University of California, Berkeley
94720

SELF-SYNCHRONIZATION OF MANY COUPLED OSCILLATORS

M. de Sousa Vieira, A. J. Lichtenberg and M. A. Lieberman

Department of Electrical Engineering and Computer Sciences
and the Electronics Research Laboratory
University of California
Berkeley CA 94720

ABSTRACT

We investigate the synchronization to a common frequency and phase in systems of many coupled digital phase locked loops. We study cases where the internal frequencies are identical for all loops and when they are different. In both cases we observe that synchronization to a common frequency is possible in a range of the parameter space. We find an analytical expression for the synchronization frequency when the communication between loops is in two directions. Synchronization in phase occurs only when the internal frequencies of the loops are identical. We study the transient convergence to the locked state in the ring, double ring and global coupling configurations. We also discuss the influence of a multiperiodic or chaotic loop on the dynamics of the system. Our results may have applications to the problem of network synchronization.

I. INTRODUCTION

Coupled oscillators are common in many scientific areas, including communications, optics, engineering, chemical reactions, biology, etc. This type of system has attracted much attention (see, for example, [1-6] and references therein), beginning with Winfree[1] who discovered that a class of coupled oscillators with different internal frequencies suddenly synchronize to a common frequency when the coupling between oscillators exceeds a critical value. Winfree and others suggested that these models could give insight into the behavior of coupled biological rhythms, such as swarms of fireflies that flash in synchrony, synchronous firing of cardiac pacemaker cells, groups of women whose menstrual cycles become synchronized, etc.[1]

The synchronization of oscillators has important practical applications in electronic systems. For example, in the design of microwave systems the power of many devices may be combined through synchronization to achieve power that increases quadratically with the number of oscillators. In this case the oscillators must have not only the same frequency, but should also have a phase difference small compared to 2π. Similar needs are found in electrical power generators, coupled lasers, Josephson junction arrays, etc. Another important application of synchronization is related to a network of clocks distributed geographically in different locations, where it is necessary to have the same time for all clocks. For this type of application, electronic devices such as phase locked loops (PLL's) have been studied [7].

In most of the previous work on self-synchronization of coupled oscillators it has been assumed that the coupling between them is smooth, that is, their dynamics is governed by ordinary differential equations. This is the case of PLL's[7] and some models for biological rhythms[1-5]. Recently a new model was introduced where the interactions between oscillators are episodic[6]. It was shown that in this model the oscillators can synchronize if they have identical internal frequencies. Here we study coupled digital phase locked loops (DPLL's) where the interactions are also episodic. However, we find that the oscillators can synchronize even when they have different internal frequencies.

The study of DPLL's started with Gil and Gupta [8]. They showed that a single first order DPLL is governed by a nonlinear difference equation, which displays regular and chaotic behavior. After this work, some studies on DPLL's have been reported[8-11], but always limited to a single loop, where the interest is the synchronization of the loop to the phase and frequency of a periodic incoming signal. Recently we have studied the self-synchronization of coupled DPLL's[12,13]. We investigated a system of two coupled loops and found regions of periodic, quasiperiodic and chaotic behavior; the boundaries between synchronized and chaotic orbits were also determined in our work.

Here we consider the problem of large networks of DPLL's. We study networks with and without variability in their component elements. Our attention is concentrated on

three types of geometries, namely, ring, double ring and global coupling. The paper is organized as follows: In section II we review the properties of one and two coupled DPLL's, and present new results for the coupled system. In section III we develop the formalism for many interconnected devices in the three configurations mentioned above. In section IV we investigate the effect of a biperiodic or chaotic loop in the network of DPLL's. Section V gives the conclusions and discussion of problems to be considered.

II. ONE AND TWO LOOPS

A single, first order, digital phase locked loop consists of a sample and hold (SH) and a variable frequency oscillator (VFO). A schematic representation of a DPLL can be seen in Fig. 1. The VFO runs with an internal frequency Ω in the absence of an input signal. Its output is given by $v(t) = A\sin\omega t$, where ω is its instantaneous frequency. When $v(t) = 0$ with a positive slope, the VFO sends a signal to the SH and a sample $v(t_k)$ is taken from the input signal. The frequency of the VFO at this instant is adjusted according to

$$\omega' = \Omega + bv(t_k), \tag{1}$$

where b is the gain of the VFO. As a consequence there is possibility of locked behavior when the VFO samples at a constant phase value. In the original papers on DPLL's[8,9] the period, not the frequency, was adjusted according to a linear function of the sampled value. However, the case we consider here is easier to implement in laboratory experiments[11,13].

The dynamical behavior of a single DPLL, governed by Eq. (1), was studied in detail in [10,11]. It was shown that when the input signal of a single loop is a sinusoid with frequency ω and amplitude A, then the time evolution of the phase difference between the input signal and the VFO output is described by the circle map

$$\phi(t_{k+1}) = \phi(t_k) + \frac{2\pi\omega}{\Omega + bA\sin\phi(t_k)}, \tag{2}$$

This map belongs to a family of circle maps which have been studied extensively in the past[14]. It exhibits periodic, quasiperiodic and chaotic behavior.

We will be concerned in this paper with coupled DPLL's, where the input of a loop is given by a combination of the outputs of the other loops. Each loop i has its own set of parameters Ω_i and b_i. We start by analyzing two coupled DPLL's where the input to one loop is the output of the other loop, and vice-versa. This system was investigated in [12] for the case where the loops have the same internal frequency. Here we study the more general case where the loops can have different internal frequencies, as well as distinct gains. A schematic representation of the system is shown in Fig. 2. In the dynamical

evolution, every time that one of the VFO signals crosses zero with a positive slope this oscillator sends a signal to its SH and a sample is taken from the output of the other loop. The loop that samples switches its frequency to a new value determined by Eq. (1).

The equations that govern the dynamics of the loops are

$$\omega_1' = \Omega_1 + b_1 A_2 \sin\phi_2, \quad (\phi_1 = 0), \tag{3a}$$

$$\omega_2' = \Omega_2 + b_2 A_1 \sin\phi_1, \quad (\phi_2 = 0). \tag{3b}$$

The gain b_i of the VFO i appears always multiplied by the amplitude A_j $(j \neq i)$ of the input signal. Thus without loss of generality we can take $A_j = 1$. Also, dividing both equations by one of the center frequencies, say Ω_2, the parameters and variables become dimensionless. We keep the same notation and simply take $\Omega_2 = 1$, having in mind that now we are working with normalized dimensionless quantities. In this way, we have

$$\omega_1' = \Omega_1 + b_1 \sin\phi_2, \quad (\phi_1 = 0), \tag{4a}$$

$$\omega_2' = 1 + b_2 \sin\phi_1, \quad (\phi_2 = 0). \tag{4b}$$

We consider that the gains are positively defined. Since the frequencies of these time discrete systems are also positive we must have $b_1 \leq \Omega_1$ and $b_2 \leq 1$. The initial condition necessary to evolve the system is the phase difference between loops, because the initial frequencies are their respective center frequencies, if we consider that before $t = 0$ the loops were uncoupled.

When the loops synchronize to a common frequency ω_s we have $\omega_1 = \omega_2 \equiv \omega_s$ and $\phi_1(\phi_2 = 0) = -\phi_2(\phi_1 = 0) \equiv \Delta\phi_s$. Putting this into Eqs. (4), we obtain

$$\omega_s = \frac{\Omega_1/b_1 + 1/b_2}{1/b_1 + 1/b_2} \tag{5}$$

and

$$\Delta\phi_s = \sin^{-1}\left(\frac{\Omega_1 - 1}{b_1 + b_2}\right). \tag{6}$$

From Eq. (6) one also sees that the synchronization is possible only if

$$b_1 + b_2 \geq |\Omega_1 - 1|. \tag{7}$$

If $b_1 + b_2$ is smaller than the critical value determined by Eq. (7), then the synchronization does not occur, and quasiperiodic behavior is observed. As b_1 and/or b_2 increase, bifurcations to higher period orbits are observed, which are followed by a chaotic regime.

The parameter values where the first bifurcation occurs can be obtained analytically via a linear stability analysis[13]. The dynamics of the locked state is governed by the eigenvalue

$$\lambda = \frac{2\pi}{2\pi - \Delta\phi_s} - \frac{2\pi(b_1 + b_2)\cos\Delta\phi_s}{\omega_s} + \frac{b_1 b_2 \Delta\phi_s(2\pi - \Delta\phi_s)\cos^2\Delta\phi_s}{\omega_s^2}, \tag{8}$$

where ω_s and $\Delta\phi_s$ are given by Eqs. (5) and (6), respectively. The synchronized state is stable if $|\lambda| < 1$ and Eq. (7) is also satisfied. When $\lambda = 0$ the system has its maximum stability. In this situation the orbit is called superstable. At $\lambda = -1$ the first bifurcation occurs. There are two possible solutions for the phase difference between the loops satisfying Eq. (6), namely, ϕ_s and $\pi - \phi_s$; however, as discussed in [13], the second one is unstable, because it always gives $\lambda > 1$. If the center frequencies of the loops are identical, that is, $\Omega_1 = \Omega_2 = 1$, then the above expression for the bifurcation point simplifies to $b_1^* + b_2^* = 1/\pi$, since $\omega_s = 1$ and $\Delta\phi_s = 0$. The maximum stability is attained at $b_1^s + b_2^s = 1/(2\pi)$, where the superscript symbol indicates the superstable value.

For small deviations from the equilibrium the transient time the system takes to synchronize can be estimated in the following way. Let $\Delta\phi_0$ denote the initial phase difference between the two loops, and $\Delta\phi_n$ the phase difference at the n-th iteration. In the linear approximation the distance from the fixed point $\epsilon_n = |\Delta\phi_n - \Delta\phi_s|$ evolves according to

$$\epsilon_n = \epsilon_0 |\lambda|^n, \tag{9}$$

where λ is given by Eq. (8). Then we have

$$n \approx \frac{\log(\epsilon_n/\epsilon_0)}{\log|\lambda|} \tag{10}$$

From Eq. (8) we find that for b_1 and b_2 fixed λ is greater in a system where the two center frequencies are different, when compared with the same quantity in a system where they are identical. Consequently, from Eq. (10) we find that the transient is smaller in the first case.

We show in Fig. 3 an example of a bifurcation diagram for a coupled loop system where we consider $b \equiv b_1 = b_2$ and $\Omega_1 = 1.2$. The quantity plotted is ω_1 vs. b. As b increases we observe a quasiperiodic regime, which is followed by a synchronized regime, bifurcations, and chaos. Eqs. (7) and (8), with $|\lambda| = 1$, correctly determine the beginning and end, respectively, of the stability of the synchronized regime. We have evolved our system numerically according to the algorithm given in [11,12].

In [12] we investigated the bifurcation sequence that precedes the chaotic regime for a system where the center frequencies of both loops were identical. We found that the period doubling bifurcation that precedes the chaotic regime is governed by Feigenbaum's exponents, which are identical to the exponents observed in the logistic map [15].

In Fig. 4 we show the regions in the b vs. Ω plane where the motion is periodic for the case where the coupling between the loops has the same strength in both directions, that is, $b \equiv b_1 = b_2$. We characterized the motion as periodic (white part) if after 1000 iterations the orbit returns to the initial point within a radius of $\epsilon = 10^{-6}$. A transient of 3000 iterations was discarded. The regular motion can be characterized by a winding number W defined by[14]

$$W = \lim_{t \to \infty} \frac{\phi_1(t) - \phi_1(0)}{\phi_2(t) - \phi_2(0)} \tag{11}$$

In the case of a periodic orbit the winding number is a rational; if the motion is quasiperiodic it will be an irrational number. The regions of periodic motion form the so-called "Arnold tongues" and are labelled in Fig. 4 by the corresponding winding numbers. Quasiperiodic motion is expected to be present in the region where b is small. The tongue 1/1 is the one where the loops are in synchrony to a common frequency, and its limiting borders are determined by Eqs. (6) and (8) with $\lambda = -1$.

III. MANY COUPLED OSCILLATORS

We now turn our attention to populations of many coupled oscillators. In such a system, every time that a VFO signal crosses zero with a positive slope the SH in that loop takes a sample from the combined outputs of the other VFO's to which it is connected. The input to the i-th sampler is assumed to be given by a linear combination of the VFO outputs of the other loops, that is,

$$s(t_i) = \frac{1}{n_i} \sum_{j=1}^{N} a_{ij} v(\phi_j(t_i)), \tag{12}$$

where $n_i = \sum_{j=1}^{N} a_{ij}$ is the number of loops from which loop i receives input. The matrix $A = [a_{ij}]$ is called the interconnection matrix for the system. If loop i receives input from loop j then $a_{ij} = 1$. Otherwise $a_{ij} = 0$. We consider $a_{ii} = 0$.

The value $s(t_i)$ is used to adjust the frequency of the i-th VFO according to

$$\omega_i' = \Omega_i + b_i s(t_i). \tag{13}$$

For systems with more than two coupled DPLL's analytical expressions for the phase difference between loops and asymptotic frequencies are difficult to find for a general configuration. The results we present with respect to many coupled DPLL's follow basically from numerical simulations. However, we can easily derive the expression for the synchronization frequency for configurations where the coupling between any pair of loops is in

both directions. If synchronization in frequency occurs then we have for all loops $\omega_i' = \omega_s$. From Eqs. (12) and (13) we obtain

$$\omega_s = \Omega_i + \frac{b_i}{n_i} \sum_j a_{ij} \sin(\phi_j), \qquad (\phi_i = 0). \tag{14}$$

Using Eq. (14) and summing over all the loops, we have

$$\sum_i \frac{\omega_s - \Omega_i}{b_i/n_i} = \sum_{ij} a_{ij} \sin(\phi_j). \tag{15}$$

If between two loops that are connected the communication exists in both directions, i.e, if $a_{ij} = 1$ then $a_{ji} = 1$, then the right-hand side of Eq. (15) vanishes. This happens because in the synchronized state $\phi_j(\phi_i = 0) = -\phi_i(\phi_j = 0)$ and $\sin(\cdot)$ is an odd function. Thus the synchronization frequency can easily be obtained from Eq. (15) as a weighted average of the Ω_i's,

$$\omega_s = \frac{\sum_i \frac{\Omega_i n_i}{b_i}}{\sum_i n_i/b_i}. \tag{16}$$

This expression for the synchronization frequency remains unchanged if $\sin(\cdot)$ is replaced by any odd periodic function. Synchronization to a common frequency and phase is not always possible in coupled DPLL's, as well as in other types of coupled oscillators. It depends on the configuration of the system and on its internal parameters, as we will see in the following sections. We study two kinds of systems:

i) *Oscillators with identical center frequencies*

If all the oscillators have the same center frequency, i.e. $\Omega_i = \Omega$, then we observe synchronization for the configurations we studied in a range of the parameter space, with the phase difference between the loops being zero. From Eq. (14) we conclude immediately that $\omega_s = \Omega$, as expected. As discussed in the previous paragraphs we can make $\Omega = 1$ in our numerical calculations without losing generality.

Our studies here are concentrated in the three basic types of configurations shown in Fig. 5, that is, (a) ring, (b) double ring, and (c) global coupling. The elements of the connection matrices for these configurations are given, respectively, by: (a) $a_{ij} = 1$ if $j = i - 1$, with $a_{1,N} = 1$; (b) $a_{ij} = 1$ if $j = i \pm 1$, with $a_{1,N} = a_{N,1} = 1$; and (c)$a_{ij} = 1$ if $i \neq j$. Otherwise, $a_{ij} = 0$. We denote by N the number of loops in the system.

In this section we consider that all loops have the same gains $b \equiv b_i$. Systems with variability in the gains will be discussed in Section IV. The parameter region where the

synchronized state is stable depends on the configuration of the system. Let us say that it is stable for b in the interval $b_c < b < b^*$. When the center frequencies are all identical $b_c = 0$ in all the configurations studied. When b is larger than b^* bifurcations and chaos appear. This is in contrast with the coupled analog PLL's studied in [7] where the existence of bifurcations and chaos has not been reported. We numerically studied systems with N varying from 2 to 200 and observed the following: For the ring configuration the first bifurcation occurs always at $b_r^* = 1/2\pi$ for any number of loops. This result was derived analytically for $N = 2$ in section II. As N is increased we observe from the numerical simulations that this value remains the same. Just beyond the critical value b_r^*, there appears a periodic regime whose period is found numerically to be given by N^2. This period refers to the number of samplings that makes the system return to a given state in frequency as well as in phase difference. By further increasing the gain more complex bifurcations occur which are followed by chaos.

For a double ring system the critical gain where the first bifurcation occurs is also given by $b_d^* = 1/2\pi$, for N large. If N is odd and small, b_d^* differs from this value, converging to it as the size of the system increases, as shown in Fig. 6 (squares). As the gain increases beyond this critical value, there appears a bifurcation with period $2N$, where more than one basin of attraction is found for N sufficiently large. This bifurcation is followed by more complex bifurcations and then by a chaotic regime.

In a global coupling configuration we find numerically that b^* seems to converge for large N to $b_g^* = 1/\pi$, as seen in Fig. 6 (triangles). The attractor that follows the synchronized state has period $2N$ and has multiple basins of attraction, for N sufficiently large. Beyond this bifurcation more complex bifurcations appear as the gain is increased, which are followed by chaos.

Although the attractor for the synchronized state is the same for all the configurations, the transient time to lock strongly depends on the geometry of the system. To study the transient to the locked state when the system is slightly perturbed we do the following. We initiate the system with each loop having an instantaneous frequency equal to its respective center frequency and an initial phase randomly distributed in the interval $\phi_i \in [0, 0.05]$. We calculate the number of sampling times n per loop that brings the system to the final attractor within a radius ϵ, that is, when

$$\sqrt{\frac{1}{N}\sum_{i=1,N}(\omega_i - \omega_s)^2} \leq \epsilon. \tag{17}$$

We find that n is well approximated by the equation

$$n \approx A \log \epsilon + B, \tag{18}$$

where, as in Eq. (10), we can interpret $A = 1/\log|\lambda|$ and $B = -\log(\epsilon_0)/\log|\lambda|$, with λ the least stable eigenvalue. Here we concentrate our analysis on the transient time related

to the linear regime. If the initial perturbations are large enough the values for A and B changes as ϵ decreases, showing the crossover from the nonlinear to the linear regime, as observed in a single second-order DPLL [10]. These studies for our system are currently under investigations and will be reported in the future.

A plot of n versus ϵ generally shows some small fluctuations which can be smoothed by averaging n over some few realizations with different initial conditions. Thus we average n over 20 realizations and vary ϵ from 10^{-10} to 10^{-4}. We use a least square fit to calculate A in a 10 loop system for the ring, double ring and global couplings. The plot of A versus b over the region where the synchronized state is stable is shown in Fig. 7. In the geometries studied B is of order of A and shows the same qualitative dependence on b. Since less negative values for A and B imply smaller transients, we conclude that the system is most stable at the maximum of the curves shown in Fig. 7. The maximum occurs, both for A and B and for both double ring and global coupling geometries, at $b^s \approx b_g^*/2 \approx 0.14$, where b_g^* is the bifurcation point of a 10 loop system in the global coupling geometry. For a system of two coupled DPLL's we showed in Section II that the superstable cycle occurs exactly at $b^*/2$. This result seems to hold for a system with any number of loops with global coupling and double ring configurations. For the ring geometry, the superstable cycle occurs at $b \approx 0.8$, which corresponds approximately to $b_r^*/2$, where b_r^* is the bifurcation point in the ring geometry.

We observe that for the one-way ring and global coupling case A and B are approximately symmetric with respect to the b value where the orbit is superstable. Whereas these parameters are quite asymmetric in the double ring geometry. This happens because, although the b value for the superstable orbit is approximately the same in double ring and global coupling, the bifurcation points for the two systems are very different as Fig. 6 shows.

The goodness of the fit of n by Eq. (18) can be evaluated by the quantity $\chi^2 = \frac{1}{P}\sum_{i=1,P}[n(\epsilon_i) - A\log\epsilon_i - B]^2$, where P is the number of ϵ values used in the fitting (we use $P = 20$) . We find that on the average χ is less than 5% of A in the three geometries.

We also study the transient as a function of the size of the system. We find that in the three geometries A versus N varies as

$$A \sim N^{\alpha}. \tag{19}$$

In Fig. 8 we show A versus N for ring (circles), double ring (squares) and global coupling (triangles) with $b = 0.12$. We find that for N large enough $\alpha \approx 0$ for global coupling. Consequently, in this geometry, as N gets large the number of sampling times per loop for the system to attain the locked state within a given accuracy does not depend on the system size. On the other hand, A increases extremely fast in the one-way ring and double ring cases. We find the same value of α for these two geometries, i.e., is $\alpha \approx 2.0$, for any b in the region where the locked state is stable.

ii) *Oscillators with different internal frequencies*

We now consider populations of DPLL's which have different internal frequencies, that is, different Ω's. In this case, synchronization to a common frequency occurs over a range of the parameter space. The transition to the synchronized state occurs suddenly when the gains attain a critical value and it is similar to the transition that occurs in the oscillators studied in [1-5], which are governed by ODE's. For configurations where the communication between loops occurs in both directions the synchronizing frequency is given by Eq. (16). Now, a phase difference between loops will occur at the synchronized state. So, what we see is a weaker form of synchronization, which is called "phase locking"[6], where the oscillators run with the same frequency and a phase difference between them. For this type of system synchronization is possible only if the gains b_i are large enough. Considering that $|sin(\cdot)| \leq 1$, we obtain from Eq. (15) that in the synchronized state

$$|\frac{\omega_s - \Omega_i}{b_i/n_i}| \leq n_i \tag{20}$$

that is, for any i the relation $b_i \geq |\omega_s - \Omega_i|$ must be satisfied. From the above expressions, we find that the lower bound for b_c, where b_c denotes the critical value of b where the synchronization occurs, is given by $b = \max(|\omega_s - \Omega_i|)$.

In the configurations studied we see that, beyond the synchronized state, as the gain b increases there appears a bifurcation at a critical value b^*. More bifurcations and a chaotic regime is observed by increasing b.

We did numerical simulations for the ring, double ring and global coupling geometries with Ω randomly distributed in the interval $[1-\Delta; 1+\Delta]$, with $\Delta = 0.1$, and the gains being the same for all loops. The bifurcations that appear at b^* have period N^2, $2N$ and $2N$ for the ring, double ring and global coupling, respectively, as in the cases of the systems with identical center frequencies. We observe that a plot of b^* versus N is qualitatively similar to Fig. 6, with b^* now being slightly greater (about 3%) than the corresponding points in Fig. 6.

With respect to b_c, we find for the ring and global coupling configurations that $b_c \approx 0.12$, for N sufficiently large. For the double ring geometry b_c increases with N, and at $N \approx 13$ it collapses with b_d^*. Thus no synchronized state for N large is observed in this geometry. In other words, the double ring geometry does not sustain synchronization in frequency for large chains when there exists a variability in the internal frequencies of the loops. For $b < b_d^*$ and N large there appears a form of weak synchronization in the chain, where groups of neighboring oscillators run at the same average frequency, but not necessarily with a fixed phase relationship. In systems with a double ring configuration we

calculated the average frequency of each loop i

$$\overline{\omega}_i = \frac{1}{m_i} \sum_{j=1,m_i} \omega_j, \tag{21}$$

where m_i is the number of sampling times of loop i. We found that $\overline{\omega}_i$ presents frequency plateaux, as in the case of the oscillators studied in [16]. We illustrate this phenomenon by showing in Fig. 9, $\overline{\omega}_i$ vs. i for a system of 200 loops, $b = 0.16$ and $m_i \approx 500$. The widths of the plateaux decrease for decreasing b. Therefore, a large system with double ring geometry with a significant variability in the center frequencies may present local synchronization of the oscillators to the same average frequency, but not a time independent common frequency for all loops.

For the ring geometry, even though the number of connections is smaller than in the double ring case we always find synchronization in frequency (phase locking) for large chains in a range of b, however at the expenses of long transients to the locked state.

We calculated the transient in a similar way as we did for the system with identical center frequencies. Beginning with the system in the steady state we perturb the phases of each loop by adding a small increment randomly chosen in the interval $\Delta\phi \in [0, 0.05]$. Then we calculate the number of sampling times per loop that takes the system to a locked state within a radius ϵ defined according to Eq. (17). We observed that the average transient n also obeys Eq. (18) for the three geometries studied. We show A versus b in Fig. 10 for a particular realization of the Ω_i's distributed in the interval $[0.9, 1.1]$ specified above in a system with $N = 10$. For double ring and global couplings the maximum of A and B occurs at $b \approx 0.17$, which is half of the b value for the bifurcation point in the global coupling geometry. Now the curves of A versus b are not symmetric with respect to their maximum. For the ring geometry the most stable state occurs for b slightly greater than its corresponding b_c. We measure the goodness of the fitting χ of n versus A by Eq. (18) and find that χ is on the average less than 5% of A in the three geometries.

For global coupling we observe that the number of samplings per loop increases slightly, with some fluctuations, as N increases. For the one-way ring $A \sim N^2$, as in the cases of the systems with identical internal frequencies. The results of A versus N for the three geometries with $b = 0.13$ are shown in Fig. 11. The double ring results stop when synchronization is lost for large N.

IV. SYNCHRONIZATION TO BIPERIODIC OR CHAOTIC LOOP

In this section we investigate systems of self-synchronized DPLL's where one of the loops has its parameters changed in such a way that it becomes multiperiodic or even

chaotic. A loop can present a multiperiodic or chaotic orbit if, for example, the gain associated with that loop is large enough or if its center frequency is small enough.

We concentrate our attention on systems where the center frequencies are identical for all loops, $\Omega = 1$. We observe similar results if we vary the center frequency of one loop by a sufficient amount, keeping the gains of all loops identical. Consider the gains of the loops identical $b_i = 0.1$, with exception of one loop, say loop 1, which will have a larger b. Take for example $b_1 = 0.35$ in a chain of 10 loops. We find that for ring, double ring and global coupling, not only does loop 1 change its state, but each loop has its frequency oscillating between two values, as shown in Fig. 12. In the one-way ring geometry (Fig. 12(a)) for each loop the difference between successive loop frequencies decreases as the loop gets far from loop 1. The communication here is only in one direction and by the inherent properties of phase locked loops, the output of a loop is found to be closer to a periodic cycle than the input signal. In this way, for i large the loop is practically locked to a unique frequency. If we denote by $\Delta\omega_i$ the difference between the two asymptotic frequencies associated with loop i, $\omega = \omega_i(1)$ and $\omega = \omega_i(2)$, then we find that, for this particular value of the parameters, $\Delta\omega_i/\Delta\omega_{i+1}$ converges to 2.1905... as i increases. For the double ring case (Fig. 12(b)), for the same values of the parameters considered in the ring geometry, we also observe that all loops have a frequency with period two. The communication in this case is in two directions, and it is observed that the loops synchronize in pairs. That is, loops 2 and 9, have exactly the same output as well as the pairs 3 and 8, 4 and 7, 5 and 6. This is expected since loops 2 and 9, and the other pairs have the same input. Therefore they will have the same output. In the global coupling case, we also find that the frequencies of each loop are biperiodic. Since in this configuration, any loop, by symmetry, is equivalent to any other one, with the exception of loop 1, all the loops will have the same output, as shown in Fig. 12(c).

We can calculate the average value of the deviation of the asymptotic frequencies $\omega_i(1)$ and $\omega_i(2)$ of the loops where $i \neq 1$, with respect to their frequencies ($\omega_s = \Omega = 1$) in the locked state, that is $\Delta\overline{\omega} = \frac{1}{P(N-1)} \sum_{i=2,N} \sum_{j=1,P} |\omega_i(j) - \Omega|$, where P is two for the case of a 2-cycle. In this way, we find which configuration on the average will present the smallest deviation from the desired locked state. As expected, the global configuration presents the smallest $\Delta\overline{\omega}$, followed by the double ring and one-way ring configurations. The respective values of $\Delta\overline{\omega}/\Omega$ are 0.56%, 1.17% and 1.23%.

If we increase the gain of loop 1 in such a way that it presents a 4-cycle orbit we observe, in this case also, the other loops will present the same periodicity, i.e. period 4. Increasing the gain of the loop 1 to $b_1 = 0.7$, we find chaotic behavior for this loop, as well as for the other loops, in the three configurations considered above. We show the results of our simulations in Fig. 13. Although figures do not distinguish between quasiperiodic and chaotic motion, a more careful analysis by calculating the Liapunov[17] exponents shows

that indeed the dynamics of all loops are chaotic.

For the one-way ring configuration the amplitude of the chaotic orbit decreases as the loop index increases, as we would expect in a phase locked loop system with communication only in one direction. For the double ring configuration the loops synchronize in pairs, as in the case described above where the loops have a 2-cycle. So, even with an input that is chaotic and the initial conditions are different, due the symmetry of the configuration, a perfect chaotic synchronization is observed between loops that have the same input. Note that if another chaotic loop is added in the system, the symmetry will be broken and the chaotic synchronization between pairs of loops will not be observed. The smallest amplitude of chaotic motion is found in the loops which are the farthest from the one with large b. For the global coupling configuration, as discussed above, all the loops (excluding loop 1) are equivalent. Therefore all the loops have identical outputs. In other words, they are synchronized. In this configuration the weight of the chaotic signal in the input signal is given by $1/N$. Thus, as we increase the system size, we observe that the amplitude of the chaotic motion in the loops with $i \neq 1$ decreases.

We also calculated the quantity $\Delta\overline{\omega}$, as defined above, in order to quantitatively obtain the deviation of the loop frequencies from the frequency of synchronization in the locked state ($\omega_s = \Omega = 1$). Now, the sum over j is made on 1000 sampling times of loop i, i.e., $P = 1000$. We find that for global coupling, double ring, and one-way ring geometries, $\Delta\overline{\omega}/\Omega$ is, respectively, 0.63%, 0.97% and 1.70%. So, the global coupling is the best configuration to filter the chaotic signal.

V. CONCLUSIONS

We have shown that populations of nonuniformily sampled digital phase locked loops can synchronize with a common frequency over a range of parameters. The synchronized frequency can be obtained analytically for configurations where the coupling between the loops that are connected occurs in both directions. In common with other coupled oscillator systems, if the spread in frequencies is not too large, there are transitions with increasing coupling from quasiperiodicy to a locked state and finally to chaos.

We studied the cases where the center frequencies are identical for all loops, and when they are spread. We found for both cases that the transient from a weakly perturbed state to the synchronized state and the parameter range where it is stable depend on the configuration of the system, with the time to lock improving with the number of couplings for a fixed number of coupled devices N. The time to lock is approximately constant for large N in the global coupling geometry, whereas in the one-way ring and double ring it varies as N^2. For large N the synchronization in the double ring geometry may not occur if the center frequencies are spread. Among the geometries studied, global coupling

showed the shortest transient to the locked state and the largest parameter region where the synchronization is possible.

If the gain of one of the loops has a sufficiently large b, we found that the synchronization to a unique frequency is destroyed. If the large b loop is multiperiodic, then each loop will have the same periodicity as the loop with the large gain, but with decreased spread in frequencies. If the loop with large b is chaotic, then all other loops will also be chaotic, but with decreased frequency spread. As expected, the average spread in frequencies from a locked state is smaller if the loops are globally coupled. For global coupling all loops except for the intrinsicly chaotic one are synchronized together.

Extensions to this study include determining nonlinear transient behavior, the investigation the effect of noise in the system, a comparison of the advantages and disadvantages of analog versus digital phase locked loops for network synchronization, and experimental investigations of self-synchronized DPLL's.

ACKNOWLEDGMENTS

We thank J. Gullicksen, J. Huang, P. Khoury, R. Sherman, M. Steinberg and W. Wonchoba for useful discussions. This work was partially supported by NSF Grant ECS-8910762 and by DARPA under AFOSR Contract F49620-90-C-0065 with Loral Western Development Laboratories.

REFERENCES

[1]. A. T. Winfree, "Biological rhythms and the behavior of populations of coupled oscillators" *J. Theor. Biol.*, vol. 16, pp.15-42, 1968; A. T. Winfree, "The Geometry of Biological Time" (Springer, New York, 1980).

[2]. Y. Kuramoto and I. Nishikawa, "Statistical macrodynamics of large dynamical systems. Case of a phase transition in oscillator communities, *J. Stat. Phys.*, vol. 49, pp. 569-605, 1987.

[3]. P. C. Matthews and S. H. Strogatz, "Phase diagram of the collective behavior of limit-cycle oscillators, *Phys. Rev. Lett.*, vol. 65, pp. 1701-1704, 1990.

[4]. N. Kopell and G. B. Ermentrout, "Symmetry and phaselocking in chains of weakly coupled oscillators, *Commun. Pure Appl. Math.*, vol. 39, pp. 623-660, 1986.

[5]. H. Daido, "Scaling behavior at the onset of mutual entrainment in a population of interacting oscillators", *J. Phys. A: Math. Gen. 20*, vol. 20, pp. L629-L636, 1987.

[6]. R. Mirollo and S. H. Strogatz, "Synchronization of pulse-coupled biological oscillators", *SIAM J. Appl. Math.* vol. 50, no. 5, pp. 1645-1662, Dec. 1990.

[7]. "Phase Locked Loops", Edited by W. C. Lindsey and C. M. Chie (IEEE Press, 1986), pp. 151-209.

[8]. G. S. Gil and S. C. Gupta, "First-order discrete phase-locked loop with applications to demodulation of angle-modulated carrier", *IEEE Trans. Commun.*, vol. COM-20, pp. 454-462, June 1972; G. S. Gil and S. C. Gupta, "On higher-order discrete phase-locked loops", *IEEE Trans. Aerosp. Electron. Syst.*, vol. AES-8, pp. 615-623, Sept. 1972.

[9]. A. Weinberg and B. Liu,"Discrete Time Analyses of Nonuniform Sampling First- and Second-Order Digital Phase Lock Loops", *IEEE Trans. Commun.*, vol. COM-22, pp. 123-137, Feb. 1974; N. A. D'Andrea and F. Russo, "A binary quantized digital phase locked loop: A graphical analysis", *IEEE Trans. Commun.*, vol. COM-36, pp. 1355-1364, Sept. 1978. H. C. Osbourne, "Stability Analysis of an *N*th Power Digital Phase-Locked Loop - Part I: First-Order DPLL", *IEEE Trans. Commun.* vol. COM-28, pp. 1343-1354, Aug. 1980.

[10]. G. M. Bernstein, M. A. Lieberman and A. J. Lichtenberg, *IEEE Trans. Commun.* vol. COM-37, 1062-1070, Oct. 1989; G. M. Bernstein and M. A. Lieberman, "Secure random number generator using chaotic circuits", *IEEE Trans. Circuits Systems*, vol. 37, no. 9, pp. 1157-1164, Sept. 1990;

[11]. G. M. Bernstein, *Nonlinear Oscillations, Synchronization and Chaos*, PhD thesis, University of California, Berkeley, 1988.

[12]. M. de Sousa Vieira, A. J. Lichtenberg and M.A. Lieberman, "*Nonlinear dynamics of self-synchronized systems*", to appear in *International Journal of Bifurcation and Chaos.*

[13]. M. de Sousa Vieira, P. Khoury, A. J. Lichtenberg, M. A. Lieberman, W. Wonchoba, J. Gullicksen, J. Y. Huang, R. Sherman, and M. Steinberg, "*Numerical and experimental studies of self-synchronization and synchronized chaos*", submitted to "International Journal of Bifurcation and Chaos".

[14]. S. J. Shenker, "Scaling behavior in a map of a circle into itself: empirical results", *Physica* (Utrecht) vol. 5D, pp. 405-411, 1982; M. J. Feigenbaum, L. P. Kadanoff, and S. J. Shenker, "Quasiperiodicity in dissipative systems: a renormalization group analysis", *Physica* (Utrecht), vol. 5D, pp. 370-386, 1982; M. H. Jensen, P. Bak, and T. Bohr, "Transition to chaos by interaction of resonances in dissipative systems. I. Circle maps", *Phys. Rev. A*, vol. 30, no. 4, pp. 1960-1969, Oct. 1984.

[15]. M. J. Feigenbaum, "Quantitative universality for a class of nonlinear transformations", *J. Stat. Phys.*, vol. 19, pp. 25-52, 1978.

[16]. H. Sakaguchi, S. Shinomoto, and Y. Kuramoto, "Local and Global Self-Entrainment in Oscillator Lattices", *Prog. Theor. Phys.*, vol. 77, 1005-1010, 1987; G. B. Ermentrout and N. Kopell, "Frequency plateaus in a chain of weakly coupled oscillators", SIAM J. Math. Anal. vol. 15, no. 2, 215-237, Mar 1984.

[17]. For more information on Liapunov exponents, see for example, A. J. Lichtenberg

and M. A. Lieberman, "Regular and Stochastic Motion" (Springer, New York, 1983). We calculated the Liapunov exponent for the coupled loop using the algorithm given by A. Wolf, J. B. Swift, H. L. Swinney and J. A. Vastano, "Determining Lyapunov Exponents from a Time Series", *Physica* (Utrecht), vol. 16D, pp. 285-317, 1985.

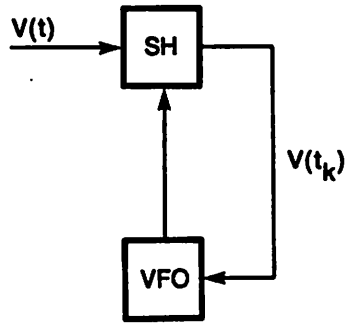

Fig. 1. Schematic representation of a single first order nonuniformily sampling DPLL.

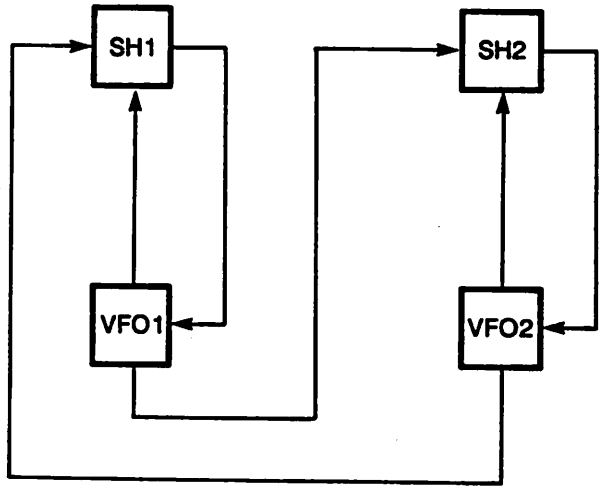

Fig. 2. Schematic representation of two self-synchronized DPLL.

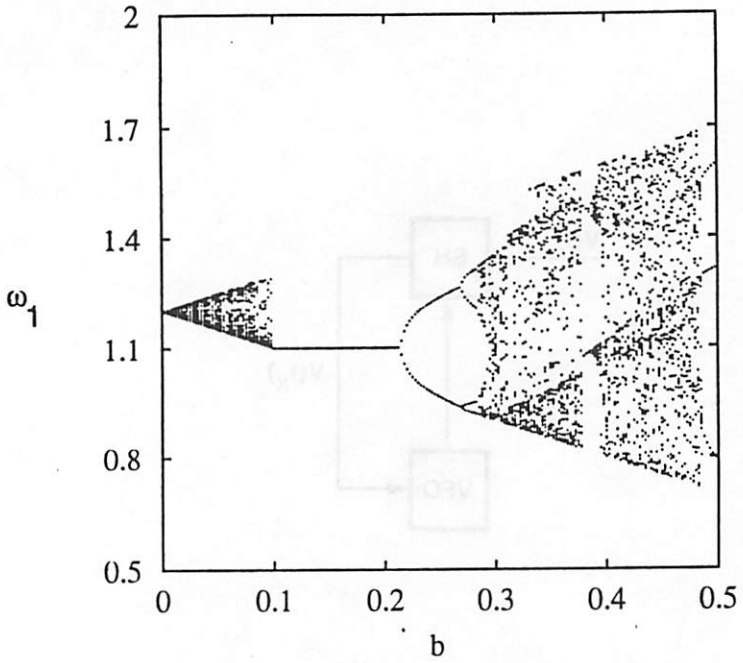

Fig. 3. Frequency of loop 1 versus $b \equiv b_1 = b_2$ for $\Omega_1 = 1.2$.

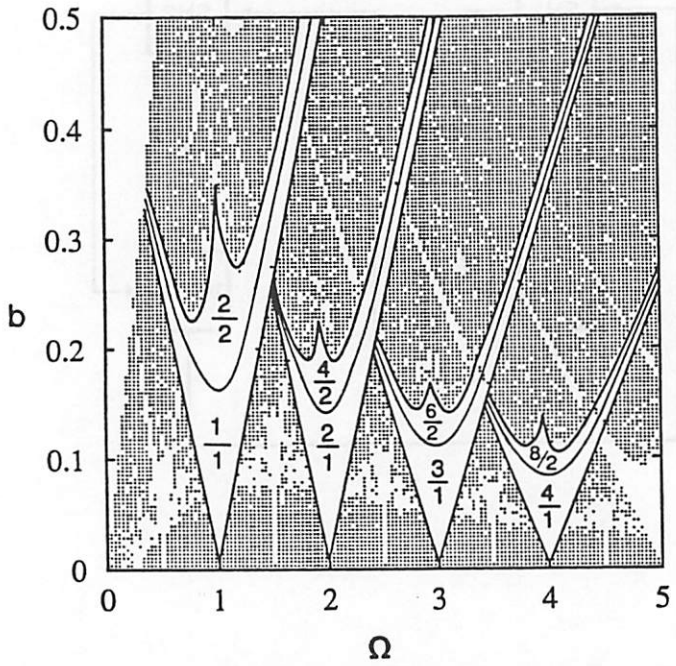

Fig. 4. Phase diagram of the two coupled DPLL with $b \equiv b_1 = b_2$. The largest "Arnold tongues" are labelled by the corresponding winding numbers.

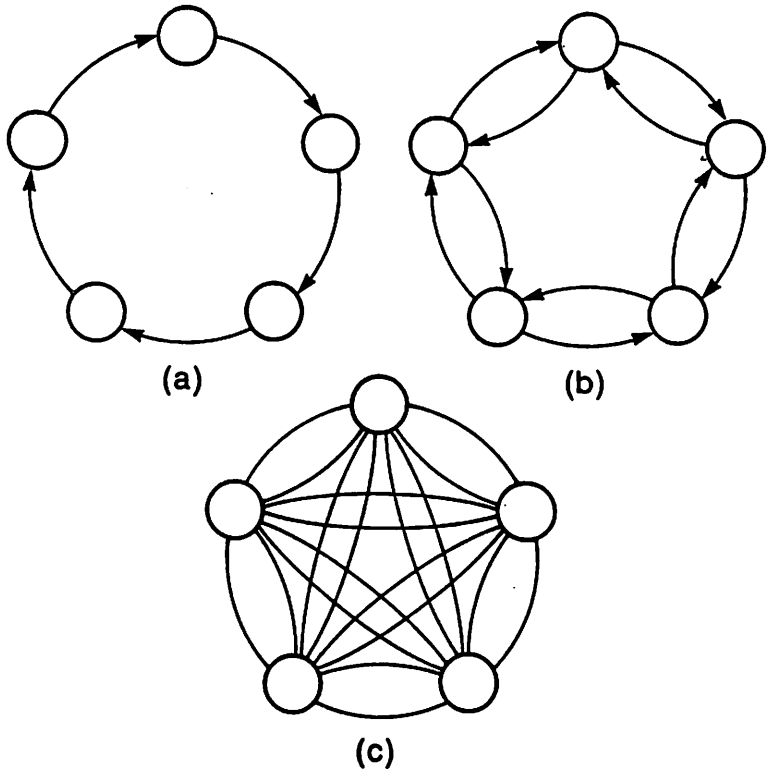

Fig. 5. Schematic representation of (a) ring, (b) double ring and (c) global coupling configurations for N=5.

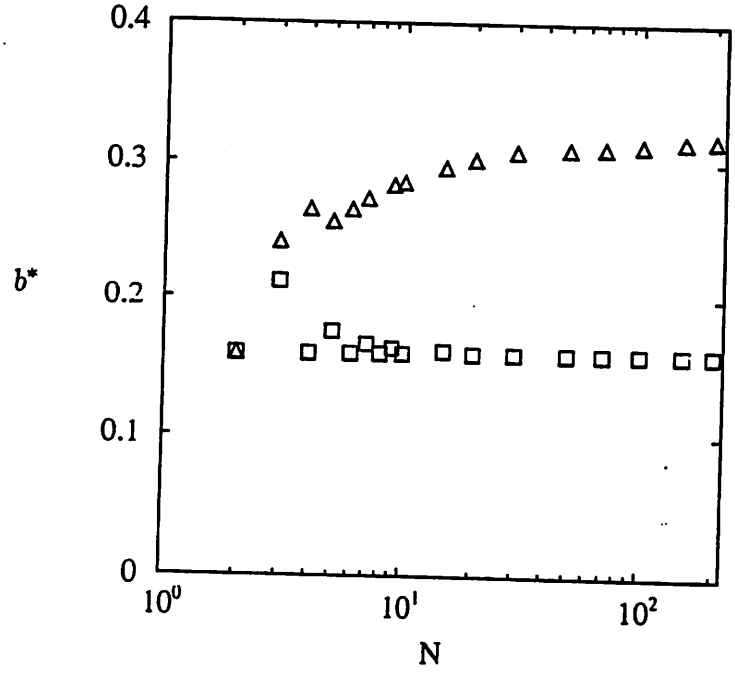

Fig. 6. Critical value b^* which marks the upper border of stability for the synchronized regime in a double ring (squares) and global coupling (triangles).

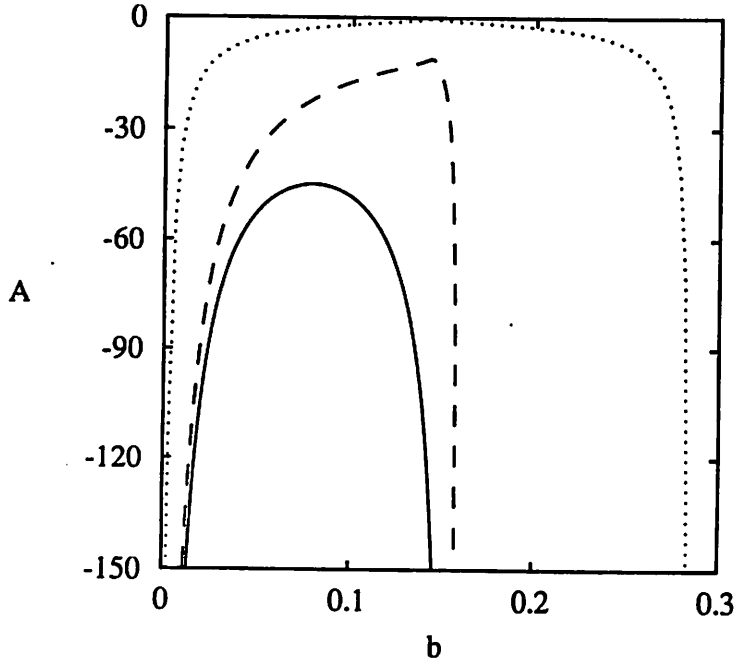

Fig. 7. A versus b for the synchronized state for one-ring (solid), double ring (dashed) and global coupling (dotted) with $\Omega_i = 1$.

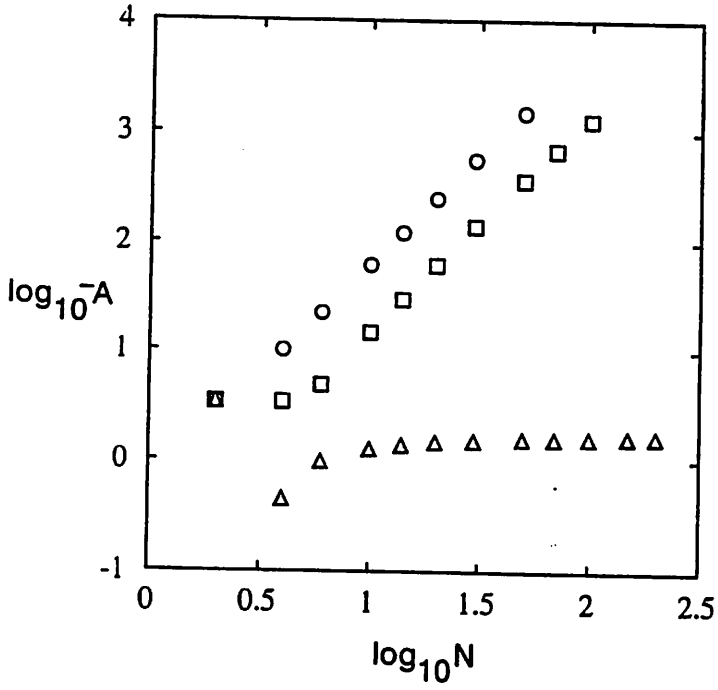

Fig. 8. A versus N for ring (circle), double ring (square) and global coupling (triangle) with $b = 0.12$.

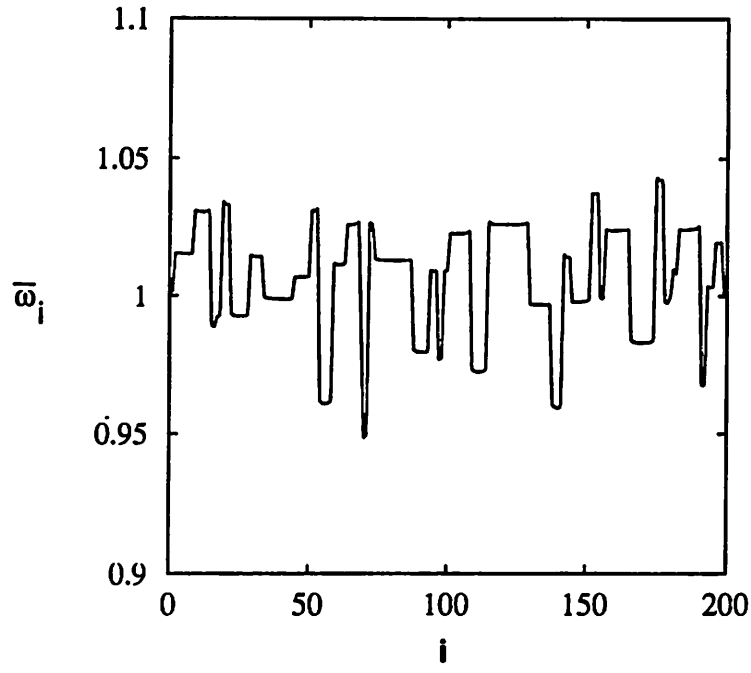

Fig. 9. Frequency plateaux for the double ring geometry, with $b = 0.16$, $N = 200$ and Ω distributed randomly in the interval $[0.9, 1.1]$.

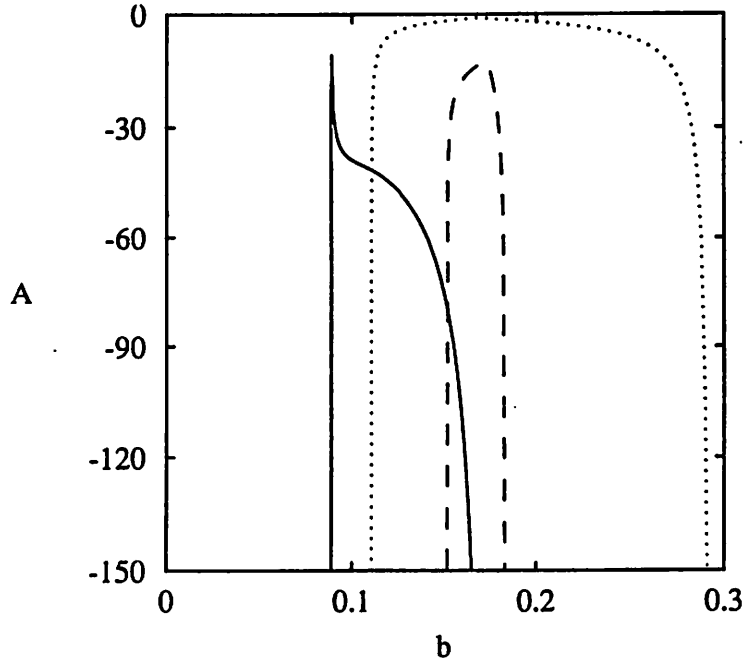

Fig. 10. A versus b for double ring (solid) and global coupling (dashed) in the synchronized state with Ω distributed in the interval $[0.9, 1.1]$.

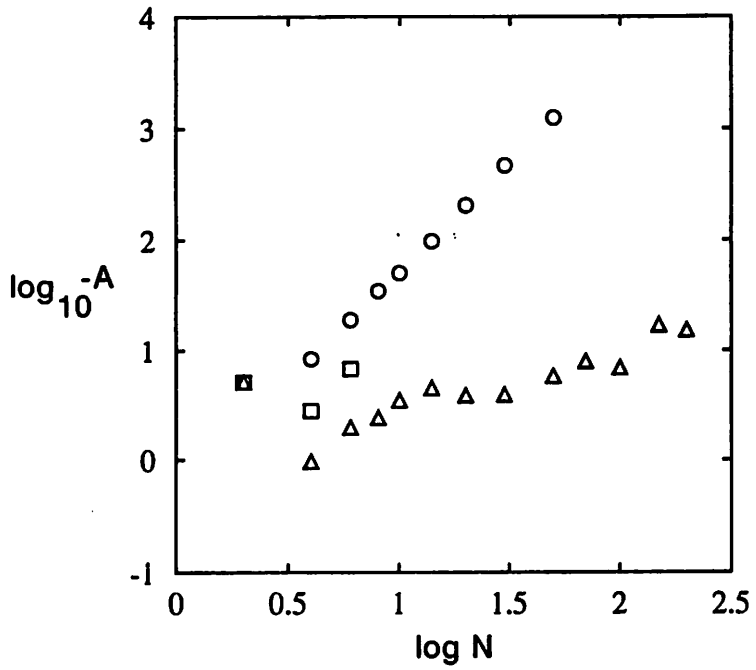

Fig. 11. A versus N for ring (circles), double ring (squares) and global coupling (triangles) with $b = 0.13$ and Ω distributed randomly in in the interval $[0.9, 1.1]$.

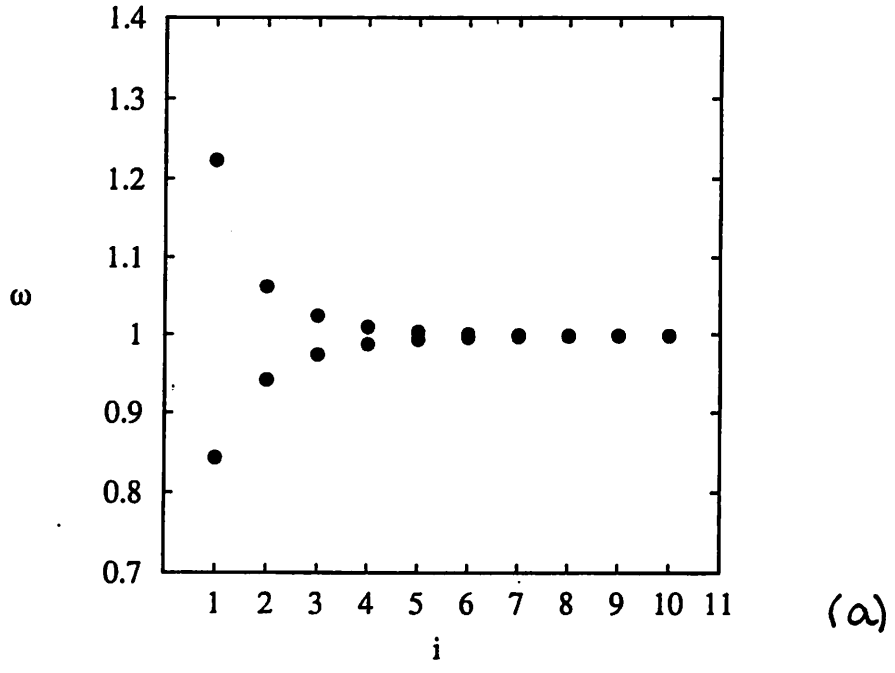

Fig. 12. Asymptotic frequencies for a system with $b_1 = 0.35$, $b_i = 0.1$ $(i = 2, N)$, $\Omega = 1$ and $N = 10$ showing the 2-cycle for (a) ring, (b) double ring and (c) global coupling.

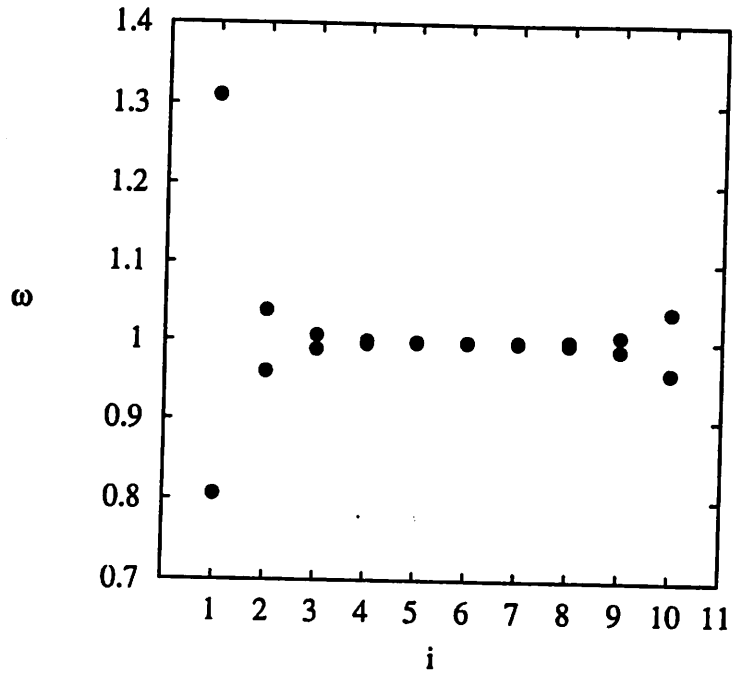

(b)

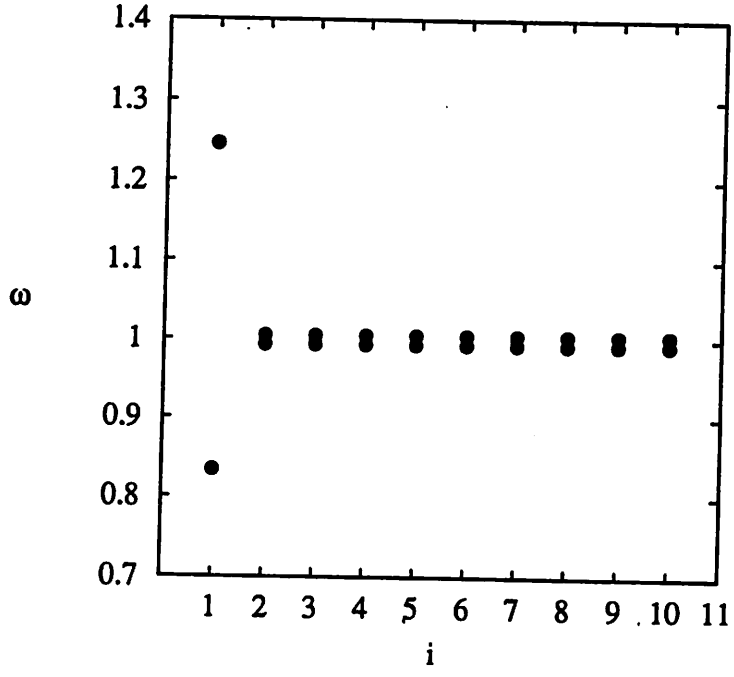

(c)

Fig. 12. (continued)

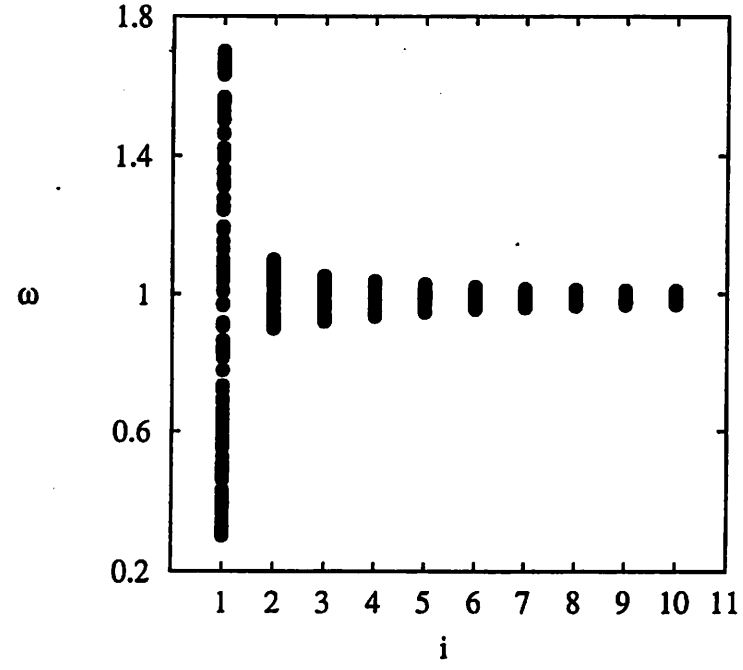

(a)

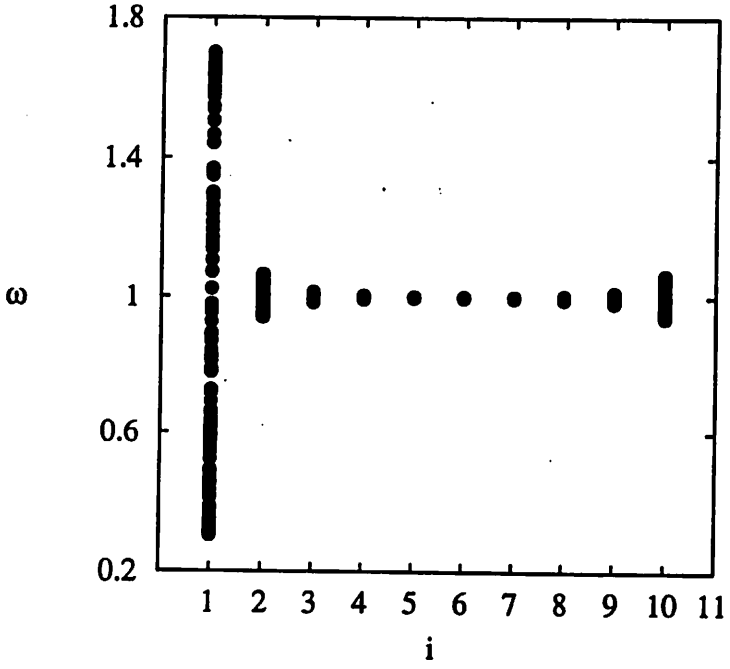

(b)

Fig. 13. Chaotic orbits for a system with $b_1 = 0.7$, $b_i = 0.1$ $(i = 2, N)$, $\Omega = 1$ and $N = 10$ showing the chaotic motion for (a) ring, (b) double ring and (c) global coupling.

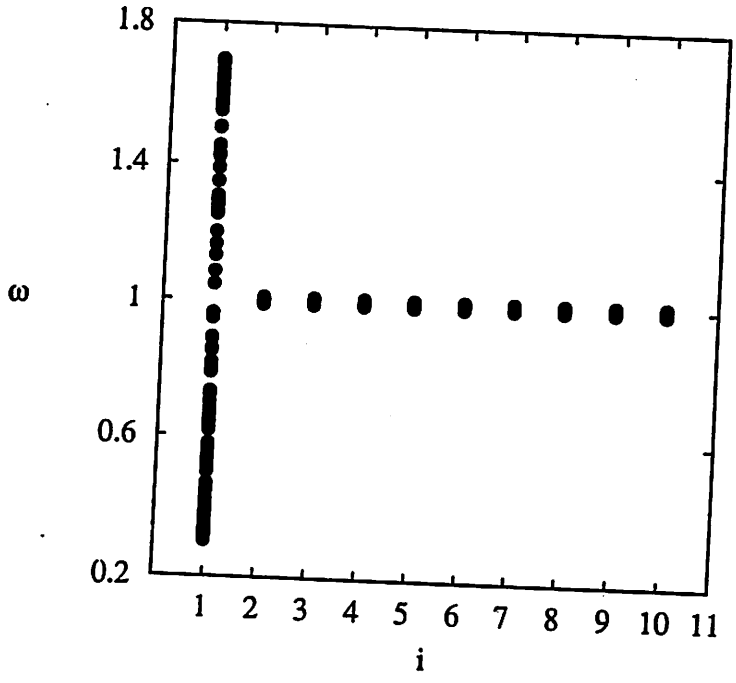

(c)

Fig. 13. (continued)